Singular meshless method using double layer potentials for exterior acoustics

D. L. Young,[a] K. H. Chen,[b] and C. W. Lee
Department of Civil Engineering and Hydrotech Research Institute, National Taiwan University, Taipei, 106 Taiwan

(Received 15 November 2004; revised 31 October 2005; accepted 1 November 2005)

Time-harmonic exterior acoustic problems are solved by using a singular meshless method in this paper. It is well known that the source points cannot be located on the real boundary, when the method of fundamental solutions (MFS) is used due to the singularity of the adopted kernel functions. Hence, if the source points are right on the boundary the diagonal terms of the influence matrices cannot be derived. Herein we present an approach to obtain the diagonal terms of the influence matrices of the MFS for the numerical treatment of exterior acoustics. By using the regularization technique to regularize the singularity and hypersingularity of the proposed kernel functions, the source points can be located on the real boundary and therefore the diagonal terms of influence matrices are determined. We also maintain the prominent features of the MFS, that it is free from mesh, singularity, and numerical integration. The normal derivative of the fundamental solution of the Helmholtz equation is composed of a two-point function, which is one of the radial basis functions. The solution of the problem is expressed in terms of a double-layer potential representation on the physical boundary based on the potential theory. The solutions of three selected examples are used to compare with the results of the exact solution, conventional MFS, boundary element method, and Dirichlet-to-Neumann finite element method. Good numerical performance is demonstrated by close agreement with other solutions. [DOI: 10.1121/1.2141130]

PACS number(s): 43.28.Js [SFU] Pages: 96–107

I. INTRODUCTION

For practical engineers, the boundary element method (BEM) has been more useful than the finite element method (FEM) during the last two decades, since the model setup takes less time for one-dimension reduction. Science and engineering communities have recently started paying attention to meshless methods that are element free. For the foreseeable future this mesh reduction technique will provide a significant and promising alternative to dominant numerical methods such as the FEM and BEM. Since neither domain nor surface meshing is required for the meshless methods, they could be more attractive for engineers to use. In this paper, we will develop a singular meshless method (SMM) as an efficient and novel numerical technique for solving two-dimensional (2D) exterior acoustics.

The mesh-free methods have become popular tools for scientific computing in recent years because of the strong demand for the reduction of mesh generation in higher dimensional domains. These methods are considered as promising alternatives to the FEM and BEM in solving physical problems numerically. Meshless methods have been successfully applied to some realistic problems[1] but not previously in acoustics. Several important types of meshless methods with their applications have been reported in the literature.[2–15,1,16–20]

Among the above-mentioned mesh-free studies, the method of fundamental solutions (MFS) is extensively applied to solve certain engineering problems.[11,13,17–19] The MFS is one kind of meshless method, since only boundary nodes are needed. Comprehensive reviews of the MFS were published by Fairweather and Karageorghis[11] and Golberg and Chen.[13] In order to avoid the problem of singularity, the solution is presented as a set of single layer potentials (corresponding to the fundamental solutions) on a nonphysical boundary (namely a fictitious boundary). The unknown densities of the fundamental solutions are determined in such a way that the boundary conditions (BCs) are satisfied by the method of collocation. The kernel function is composed of a two-point function that is one kind of radial basis function (RBF). A regular meshless formulation and singularity-free method are then obtained, which are attractive and relatively easy to use. However the MFS has not become a popular numerical method because it involves a controversial artificial boundary outside the physical domain. In general a fictitious boundary is difficult to choose for a complicated geometry. This will produce a restriction on the implementation of the MFS, since the locations of the source points require good estimates. The diagonal coefficients of the influence matrices are divergent in common cases when the off-set boundary approaches the real boundary. Despite the lack of singularities, the influence matrices become ill posed when the off-set boundary is far away from the real boundary. The results become very sensitive, since the condition number gets very large.

[a]Electronic mail: dlyoung@ntu.edu.tw
[b]Present address: Department of Information Management, Toko University, No. 51, Sec. 2, University Road, Pu-Tsu, Chia-Yi, 613, Taiwan.

An improved approach called the boundary knot method (BKM) or the boundary collocation method (BCM) was introduced recently by Chen and co-workers,[3–8] Kang and collaborators,[14,15] and Chen and co-workers.[9,10] Nonsingular kernels were employed to evaluate the complementary solutions instead of using singular fundamental solutions. Many types of problems have been successfully treated with these methods. The major differences between the nonsingular schemes and MFS formulations are that the BKM and BCM choose nonsingular general solutions while MFS uses more effective singular kernel functions such as the RBFs. The Trefftz method is also one improved method for MFS. The Trefftz method uses the complementary set of fundamental solutions, i.e., the solutions of homogeneous differential equations. Hence it does not encounter the singularity since the RBFs are regular. On the other hand the MFS uses fundamental solutions of inhomogeneous differential equations which are appropriate as well. It is worth noticing that MFS and the Trefftz method are mathematically equivalent in spite of their essentially minor and apparent differences in formulation. The link between the Trefftz method and the MFS has been discussed in detail in Refs. 6 and 7. The study on the similarities between the Trefftz method and the MFS has been emphasized recently.

In the above-mentioned references, these methods only work well in regular geometry with Dirichlet and Neumann BCs. Even though those methods can locate the source points on the physical boundary and have nonsingular kernels, it still is an ill-posed problem. Further, for exterior acoustics problems the satisfaction of the BC at infinity such as Sommerfeld radiation condition becomes difficult. However the singular kernel functions for the MFS and proposed SMM will automatically satisfy the Sommerfeld radiation condition. The goal of this paper is to develop a new meshless method with the source points on the physical boundary to solve scattering and radiation problems without the above-mentioned difficulty of BKM, BCM, conventional MFS, and the Trefftz method. We present an alternative approach for the numerical treatment of exterior acoustics, retaining the salient MFS meshless characteristics and selecting the normal derivative of the fundamental solution of the Helmholtz equation as the RBF. The proposed method can be viewed as a special case of indirect BEM using the discrete double layer potential method[21–23] as well as an expansion method of the MFS.[20] The solution of the problem is expressed in terms of a double-layer potential instead of a single-layer potential representation on the physical boundary without the integral process. By comparison with other meshless or mesh reduction schemes such as BKM, BCM, or BEM, the discretization processes or regularization techniques are still needed for those methods and can be found in Refs. 22–25. However the proposed SMM behaves like the MFS by improving the singularity evaluation of diagonal terms, when the source and boundary points are coincident to avoid the ambiguity of off-set distance of the fictitious boundary for the conventional MFS.

By using the proposed regularization technique of subtracting and adding-back, the singularity and hypersingularity of the kernel functions can be regularized. The main idea is to add one singular term in the series and then to subtract the same singular term from the series of the solution representation. The two singular terms are equal and the sum of the augmented series is zero. In general the diagonal terms of the influence matrices can then be derived by using the proposed technique for an arbitrary domain. Also, the influence coefficients for a circular domain are computed analytically by using separable kernels and circulants, and the validity of the diagonal terms can be verified by using the proposed regularization technique. The main part of this paper deals with the strongly singular and hypersingular kernel functions without integration. Furthermore, the innovative concept of this study is that this regularization technique has never been used in the context of meshless methods, except for the writers' recent publication on potential problems.[20] Finally, we present several case studies using the developed singular meshless program to demonstrate that the proposed scheme can be utilized to solve 2D acoustic radiation and scattering problems in circular and square domains subject to Dirichlet and Neumann BCs.

II. FORMULATION

Acoustic problems are usually modeled by the Helmholtz equation. By making the time harmonic assumption, $p(\mathbf{x},t)=\mathrm{Re}\{\phi(x)e^{i\omega t}\}$, the classical wave equation then reduces to the Helmholtz equation as follows:

$$\nabla^2\phi(x)+k^2\phi=0, \quad x\in D^e \tag{1}$$

with the two kinds of BCs as

$$\phi(x)=\bar{\phi}, \quad x\in B \tag{2}$$

or

$$\psi(x)=\bar{\psi}, \quad x\in B, \tag{3}$$

where ∇^2 is the Laplacian, $\phi(x)$ is the acoustic pressure, $\psi(x)=\partial\phi(x)/\partial n_x$ is the normal derivative, n_x is the outward normal vector, k is the wave number, and D^e is the domain of the exterior problem. The two BCs in Eqs. (2) and (3) are stated as follows: Eq. (2) is the essential boundary (Dirichlet boundary) on which the potential is prescribed as $\bar{\phi}$ and Eq. (3) is the natural boundary (Neumann boundary) on which the flux is prescribed as $\bar{\psi}$. B is the boundary of the domain D^e. Furthermore, in order to obtain a well-posed problem; the pressure field is constrained to vanish at infinity. This is accomplished by imposing a radiation condition at infinity. An appropriate radiation condition at infinity is given by the Sommerfeld radiation condition[23,26] as

$$\lim_{r\to\infty} r^{(1/2)(d-1)}\left(\frac{\partial\phi}{\partial r}-ik\phi\right)=0, \quad r\to\infty, \tag{4}$$

where d is the dimension ($d=2$ in this study). Equation (4) stems from the Sommerfeld radiation condition which ensures that no sources at infinity contribute to the acoustic field. Only outgoing traveling waves are acceptable, guaranteeing a net acoustic energy flow toward infinity. This BC implies an integral form, the Rellich–Sommerfeld radiation condition in the form

$$\lim_{r\to\infty}\int_{B_r}\left|\frac{\partial\phi}{\partial r}-ik\phi\right|^2 dB=0, \tag{5}$$

where B_r is the surface of a sphere with a radius r. The radiation condition requires the energy flux at infinity to be positive, thereby assuring a unique solution to the boundary-value problem (1)–(4). Appropriate representation of this condition is crucial to the reliability of any numerical formulation of the problem. A correct and exhaustive presentation of the radiation decay condition has been given in Ref. 27.

By employing the RBF technique, the solution for an exterior problem can be approximated in terms of the strengths of the singularities (s^j) as

$$\phi(x^i)=\sum_{j=1}^{N}A^e(s^j,x^i)\alpha^j,\quad x\in D^e, \tag{6}$$

$$\psi(x^i)=\sum_{j=1}^{N}B^e(s^j,x^i)\alpha^j,\quad x\in D^e, \tag{7}$$

where $A^e(s^j,x^i)$ is the RBF in which the superscript denotes the exterior domain, α^j are the unknown coefficients, N is the number of source points, s^j, and

$$B^e(s^j,x^i)=\frac{\partial A^e(s^j,x^i)}{\partial n_x}.$$

The coefficients $\{\alpha^j\}_{j=1}^N$ are determined, such that BC is satisfied at the boundary points ($\{x^i\}_{i=1}^N$). By collocating N observation points, x^i, to match the BCs from Eq. (2) for Dirichlet problems and Eq. (3) for Neumann problems, we have the following $N\times N$ linear systems in the form of

$$\{\bar{\phi}^i\}=\begin{bmatrix}a_{1,1}&a_{1,2}&\cdots&a_{1,N}\\a_{2,1}&a_{2,2}&\cdots&a_{2,N}\\\vdots&\vdots&\ddots&\vdots\\a_{N,1}&a_{N,2}&\cdots&a_{N,N}\end{bmatrix}\{\alpha^j\}=[A^e]\{\alpha^j\}, \tag{8}$$

$$\{\bar{\psi}^i\}=\begin{bmatrix}b_{1,1}&b_{1,2}&\cdots&b_{1,N}\\b_{2,1}&b_{2,2}&\cdots&b_{2,N}\\\vdots&\vdots&\ddots&\vdots\\b_{N,1}&b_{N,2}&\cdots&b_{N,N}\end{bmatrix}\{\alpha^j\}=[B^e]\{\alpha^j\}, \tag{9}$$

where

$$a_{i,j}=A^e(s^j,x^i),\quad i,j=1,2,\ldots,N, \tag{10}$$

$$b_{i,j}=B^e(s^j,x^i),\quad i,j=1,2,\ldots,N. \tag{11}$$

The chosen RBFs are the double layer potentials from potential theory given as

$$A^e(s^j,x^i)=-\frac{i\pi k}{2}H_1^{(1)}(kr_{ij})\frac{n_k y_k}{r_{ij}}, \tag{12}$$

$$B^e(s^j,x^i)=\frac{i\pi k}{2}\left\{k(H_2^{(1)})(kr_{ij})\frac{y_k y_l n_k\bar{n}_l}{r_{ij}^2}-H_1^{(1)}(kr_{ij})\frac{n_k\bar{n}_k}{r_{ij}}\right\}, \tag{13}$$

where $H_1^{(1)}(kr_{ij})$ and $H_2^{(1)}(kr_{ij})$ are the Hankel functions of the first kind of the first and second order, respectively. $r_{ij}=\Sigma_{k=1}^2|s_k^j-x_k^i|$, $y_k n_k=\Sigma_{k=1}^2(x_k^i-s_k^j)n_k$, n_k is the kth component of the outward normal vector at source point s^j; $\bar{n}_k$ is the kth component of the outward normal vector at field point x^i. It is noted that the double layer potentials in Eqs. (12) and (13) have both singularity and hypersingularity at the origin, which lead to troublesome singular kernels and a controversial auxiliary boundary for the MFS. The off-set distance between the off-set (auxiliary) boundary (B') and the real boundary (B) needs to be chosen deliberately. To overcome this drawback, s^j is distributed on the real boundary by using the following proposed regularization techniques. The rationale for choosing the double layer potential instead of single layer potential as used in the proposed method for the form of RBFs is to take advantage of the regularization of the subtracting and adding-back technique, so that no off-set distance is needed when evaluating the diagonal coefficients of influence matrices as explained in Sec. III. The single layer potentials cannot be chosen as RBFs, because Eqs. (20) and (21) in the following text of Sec. III are not satisfied. If the single layer potential is used, the regularization technique of subtracting and adding-back will fail.

III. DERIVATION OF DIAGONAL COEFFICIENTS OF INFLUENCE MATRICES FOR AN ARBITRARY DOMAIN USING SMM

When the collocation point x^i approaches the source point s^j, Eqs. (12) and (13) will be approximated by

$$\lim_{x_i\to s_j}A^e(s^j,x^i)=\bar{A}^e(s^j,x^i)=\frac{n_k y_k}{r_{ij}^2}, \tag{14}$$

$$\lim_{x_i\to s_j}B^e(s^j,x^i)=\bar{B}^e(s^j,x^i)=\left(2\frac{y_k y_l n_k\bar{n}_l}{r_{ij}^4}-\frac{n_k\bar{n}_k}{r_{ij}^2}\right)+\frac{k^2}{4}i, \tag{15}$$

by using the limiting form for small arguments and the identities from the generalized function as shown in the following:[28]

$$\lim_{r_{ij}\to 0}H_1^{(1)}(kr_{ij})=\frac{kr_{ij}}{2}+\frac{2}{\pi kr_{ij}}i, \tag{16}$$

$$\lim_{r_{ij}\to 0}H_2^{(1)}(kr_{ij})=\frac{(kr_{ij})^2}{8}+\frac{4}{\pi(kr_{ij})^2}i. \tag{17}$$

The kernels in Eqs. (14) and (15) have the same singularity strength as the Laplace equation.[20] Therefore, Eqs. (6) and (7) for the exterior problem need to be regularized by using special treatment such as

$$\bar{\phi}(x^i) = \sum_{j=1}^{N} A^e(s^j,x^i)\alpha^j - \sum_{j=1}^{N} \bar{A}^e(s^j,x^i)\alpha^i$$
$$= \sum_{j=1}^{i-1} A^e(s^j,x^i)\alpha^j + \sum_{j=i+1}^{N} A^e(s^j,x^i)\alpha^j - \left[\sum_{m=1}^{N} \bar{A}^e(s^m,x^i) - A^e(s^i,x^i)\right]\alpha^i, \quad x^i \in B, \tag{18}$$

$$\bar{\psi}(x^i) = \sum_{j=1}^{N} B^e(s^j,x^i)\alpha^j - \sum_{j=1}^{N} \bar{B}^e(s^j,x^i)\alpha^i$$
$$= \sum_{j=1}^{i-1} B^e(s^j,x^i)\alpha^j + \sum_{j=i+1}^{N} B^e(s^j,x^i)\alpha^j - \left[\sum_{m=1}^{N} \bar{B}^e(s^m,x^i) - B^e(s^i,x^i)\right]\alpha^i, \quad x^i \in B, \tag{19}$$

where $\bar{A}^e(s^j,x^i)$ and $\bar{B}^e(s^j,x^i)$ are the double layer potentials of the exterior problem of the Laplace equation for the same domain, in which

$$\sum_{j=1}^{N} \bar{A}^e(s^j,x^i) = 0, \tag{20}$$

$$\sum_{j=1}^{N} \bar{B}^e(s^j,x^i) = 0. \tag{21}$$

The detailed derivations of Eqs. (20) and (21) are given in Appendix A. The original singular terms of $A^e(s^i,x^i)$ and $B^e(s^i,x^i)$ in Eqs. (6) and (7) have been transformed into regular terms $-[\Sigma_{m=1}^{N}\bar{A}^e(s^m,x^i) - A^e(s^i,x^i)]$ and $-[\Sigma_{m=1}^{N}\bar{B}^e(s^m,x^i) - B^e(s^i,x^i)]$ in Eqs. (18) and (19), respectively. The terms of $\Sigma_{m=1}^{N}\bar{A}^e(s^m,x^i)$ and $\Sigma_{m=1}^{N}\bar{B}^e(s^m,x^i)$ are the adding-back terms and the terms of $A^e(s^i,x^i)$ and $B^e(s^i,x^i)$ are the subtracting terms in the two brackets for the special treatment technique. After using the regularization technique of subtracting and adding-back, we are able to remove the singularity and hypersingularity of the kernel functions. Therefore, the diagonal coefficients for the exterior problem can be extracted out as

$$\{\bar{\phi}^i\} = \begin{bmatrix} \sum_{m=1}^{N} \bar{a}_{1,m} - a_{1,1} & a_{1,2} & \cdots & a_{1,N} \\ a_{2,1} & \sum_{m=1}^{N} \bar{a}_{2,m} - a_{2,2} & \cdots & a_{2,N} \\ \vdots & \vdots & \ddots & \vdots \\ a_{N,1} & a_{N,2} & \cdots & \sum_{m=1}^{N} \bar{a}_{N,m} - a_{N,N} \end{bmatrix} \{\alpha^j\}, \tag{22}$$

$$\{\bar{\psi}^i\} = \begin{bmatrix} -\left(\sum_{m=1}^{N} \bar{b}_{1,m} - b_{1,1}\right) & b_{1,2} & \cdots & b_{1,N} \\ b_{2,1} & -\left(\sum_{m=1}^{N} \bar{b}_{2,m} - b_{2,2}\right) & \cdots & b_{2,N} \\ \vdots & \vdots & \ddots & \vdots \\ b_{N,1} & b_{N,2} & \cdots & -\left(\sum_{m=1}^{N} \bar{b}_{N,m} - b_{N,N}\right) \end{bmatrix} \{\alpha^j\}, \tag{23}$$

where $a_{ij}=A^e(s^j,x^i)$, $\bar{a}_{ij}=\bar{A}^e(s^j,x^i)$, $b_{ij}=B^e(s^j,x^i)$, and $\bar{b}_{ij}=\bar{B}^e(s^j,x^i)$.

By collocating N observation points to match the BCs from Eq. (2) for Dirichlet BCs and Eq. (3) for Neumann BCs, we can get the final system of Eqs. (8) and (9). For mixed-type problems, a linear combination of Eqs. (8) and (9) is made to satisfy the mixed-type BCs. After the unknown density, $\{\alpha^j\}_{j=1}^{N}$, is solved by using the linear algebraic solver, the solutions for the domain of interest can be calculated by using the field equations (6) and (7) since the unknown density function $\{\alpha^j\}$ is solved by Eqs. (22) and (23). The numerical procedure of SMM can be found in Fig. 1.

The diagonal terms of the two influence matrices for exterior problems can also be derived analytically for a circular domain as shown in Eqs. (B21) and (B22).

IV. NUMERICAL RESULTS

In order to show the accuracy and validity of the proposed method, three case studies, involving radiation and

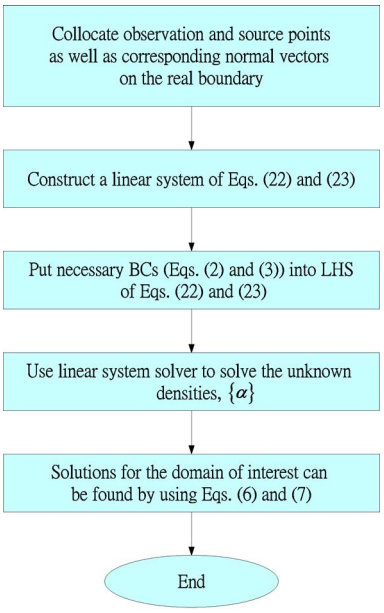

FIG. 1. (Color online) Flow chart of SMM.

scattering problems with circular and square domains subject to Dirichlet and Neumann BCs, are given in the following examples.

1. Radiation problem (Dirichlet BC). For the first case, a nonuniform radiation problem from a sector of a circular cylinder[26] is considered. The BC has a constant nonzero value on the arc $(-\alpha/2 \leqslant \theta \leqslant \alpha/2)$ and zero elsewhere. Two points of discontinuity of the BC can be found. Problem sketch and nodes distribution by using SMM are plotted in Figs. 2 and 3, respectively. The normalized analytical solution is available as follows:

$$\phi(r,\theta) = -\frac{2}{\pi}\sum_{n=0}^{\infty} \varepsilon_n \frac{\sin(n\alpha)}{n} \frac{H_n^{(1)}(kr)}{H_n^{(1)}(ka)} \cos(n\theta), \tag{24}$$

where ε_n is the Neumann factor and a is the radius of the circular cylinder. We choose $\alpha=\pi/9$. After collocating 100 nodes on the physical boundary, both the real and imaginary components for ϕ on $r=2a$ for $ka=1$ are plotted in Figs. 4(a) and 4(b), respectively. The results are used for comparison with the exact solution and the conventional Cauchy singular

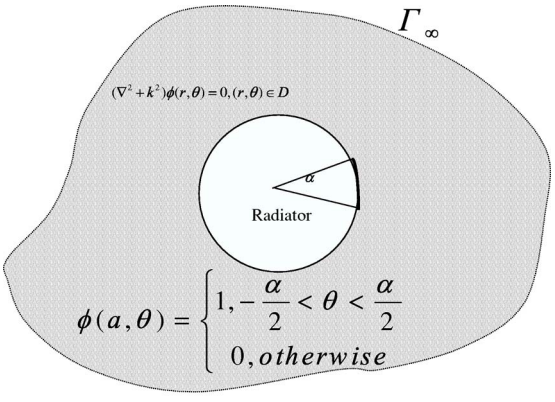

FIG. 2. The nonuniform radiation problem for a circular cylinder subject to Dirichlet BC in Case 1.

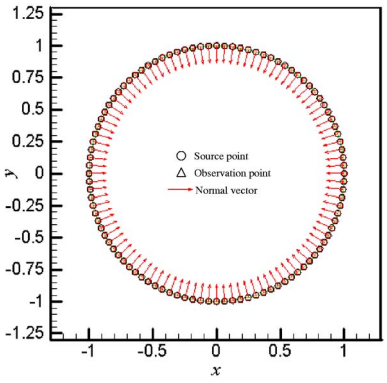

FIG. 3. (Color online) Nodes distribution (100 nodes) in Case 1.

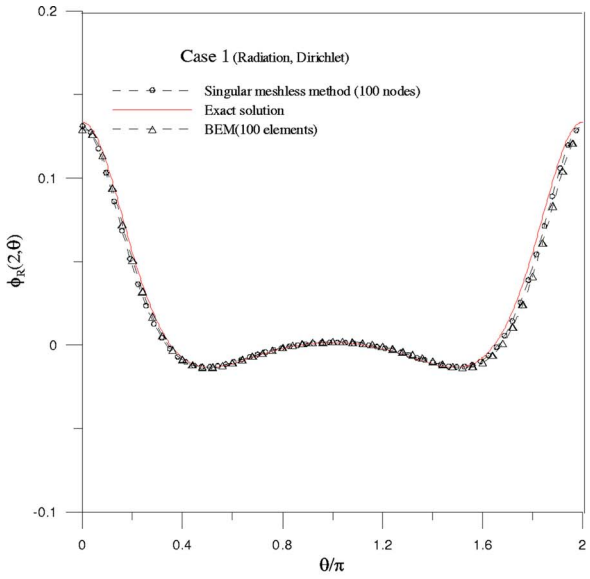

(a) Real part

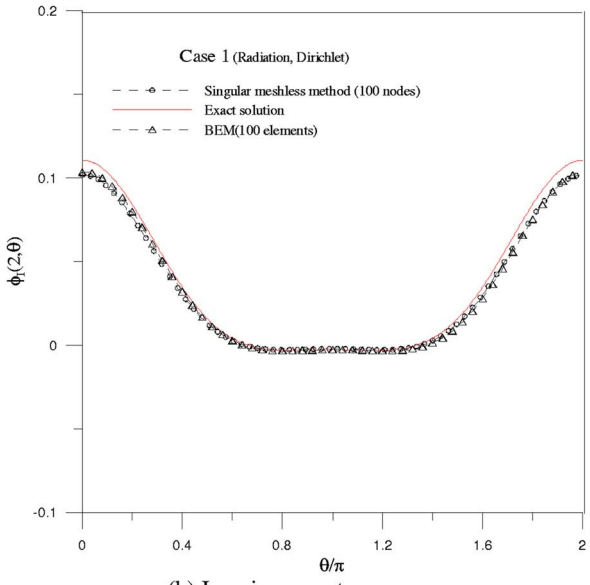

(b) Imaginary part

FIG. 4. (Color online) Nonuniform radiation for a circular cylinder subject to Dirichlet BC in Case 1 for $ka=1$, $r=2a$: (a) real part, (b) imaginary part.

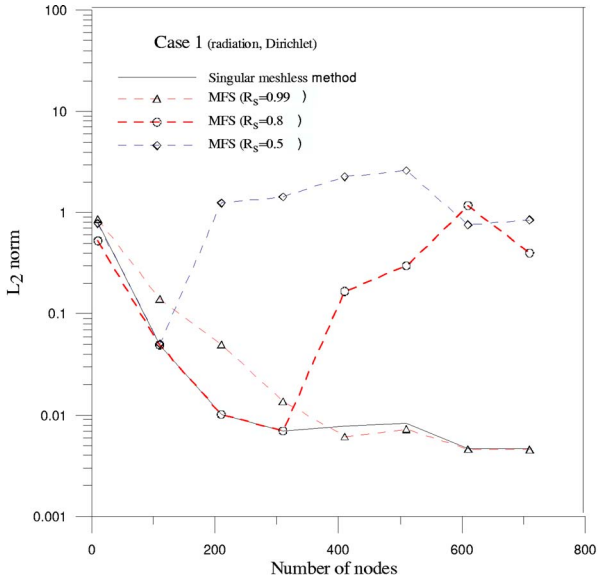

FIG. 5. (Color online) Comparison of error norms using the conventional MFS and proposed SMM for Case 1.

BEM solution. The discretization method of the BEM is collocation discretization with constant elements. These results demonstrate the convergence of the proposed method. The comparison of error norms between the present SMM using double layer potentials and the conventional MFS utilizing single layer potentials with different off-boundary distances (R_s=the radius of source points=0.5,0.8,0.99) is shown in Fig. 5. This illustrates the drawback of the location of source being dubious when the conventional MFS is used. The result using the present method is more efficient than the solution using the conventional MFS with the same number of nodes. Figures 6(a), 6(b), and 6(c) show the contour plots for the real part of the potential for $ka=1$ by adopting the analytical solution, the proposed SMM, and the BEM. The result from using the present method matches the exact solution and the BEM result very well.

2. Radiation problem (Neumann BC). The second example is the same as the first problem except the Dirichlet BC is replaced by the Neumann BC as depicted in Fig. 7. The nodes distribution employing the proposed method is shown in Fig. 8. The discontinuous BC is as follows:

$$\psi(a,\theta)=\begin{cases}1, & -\dfrac{\alpha}{2}<\theta<\dfrac{\alpha}{2}\\ 0, & \text{otherwise}.\end{cases} \tag{25}$$

In this case, the analytical solution is found as follows:[26]

$$\phi(r,\theta)=-\frac{2}{\pi k}\sum_{n=0}^{\infty}\varepsilon_n\frac{\sin(n\alpha)}{n}\frac{H_n^{(1)}(kr)}{H_n^{(1)}(ka)}\cos(n\theta), \tag{26}$$

We select $\alpha=\pi/9$. By collocating 100 nodes on the circular boundary, both the real and imaginary components for ϕ on $r=2a$ for $ka=1$ are plotted in Figs. 9(a) and 9(b), respectively. They are used for comparison with the results of exact solution and the conventional Cauchy singular BEM solution with constant elements. These results demonstrate the convergence of the proposed method. The comparison of error

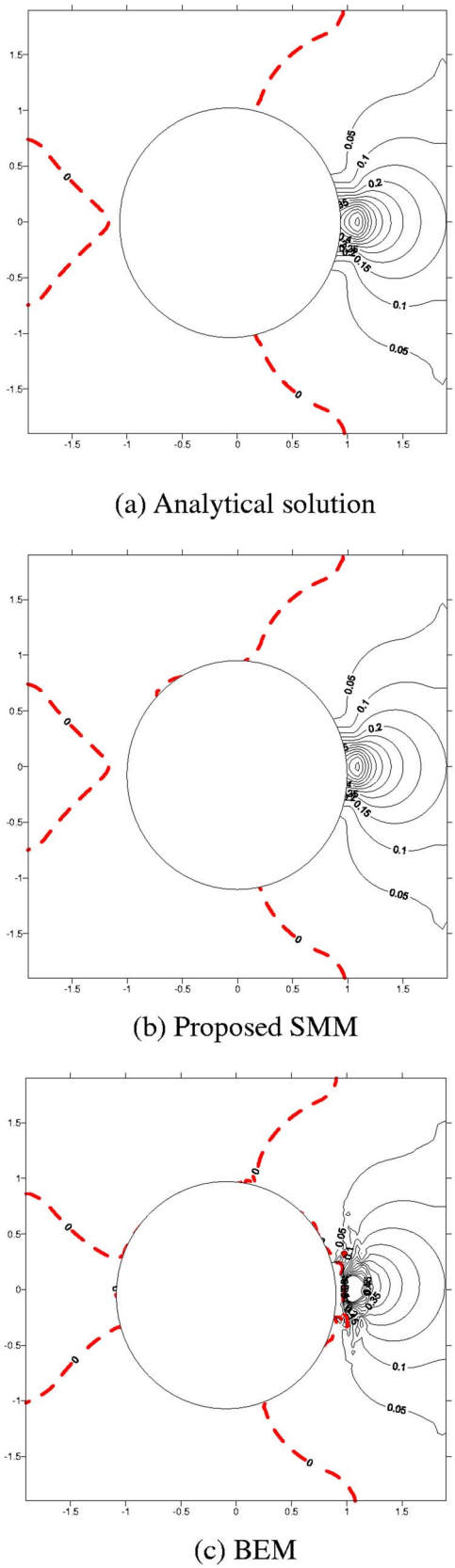

FIG. 6. (Color online) The contour plots for the real-part solutions in Case 1: (a) analytical solution, (b) proposed SMM (100 nodes), (c) BEM (100 elements).

norms between the present SMM and the conventional MFS with different off-boundary distances (R_s=0.5,0.8,0.99) is shown in Fig. 10. This illustrates again the drawback of the well known ill-posed influence matrices when the con-

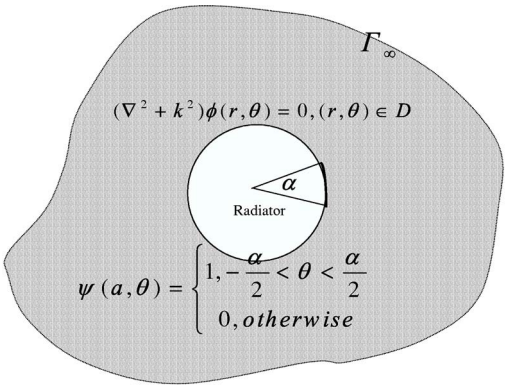

FIG. 7. The nonuniform radiation problem for a circular cylinder subject to Neumann BC in Case 2.

ventional MFS is used. The solution using the present SMM is more efficient than the conventional MFS, if the same number of nodes is used. The contour plots for the real part of the potential for $ka=1$ by adopting the analytical solution, the proposed SMM, and the BEM are shown in Figs. 11(a), 11(b), and 11(c), respectively. Figure 11 reveals that the present model provides very promising results as compared to the analytic and BEM solutions.

3. Scattering problem for a square rod (Neumann BC). Having demonstrated the present technique on a circular cylinder, we proceed to a scattering problem for a square rod (square measure=4), as shown in Fig. 12 in which the exact solution is not available.[29] Due to nonsmooth boundaries at the four corners of the square, the scattering by the square rod becomes multidirectional. By collocating 120 nodes on the square boundary as depicted in Fig. 13, both the real and imaginary components for ϕ on $r=1/0.425$ for $ka=4\pi$ are plotted in Figs. 14(a) and 14(b), respectively, for comparison with the BEM and Dirichlet-to-Neumann (DtN) FEM results. The type of finite elements used is linear triangle elements. The DtN-FEM evaluation uses the h-refinement and Galerkin least-squares finite element formulation with fully coupled DtN BCs. These results demonstrate the numerical convergence and easy treatment of BCs for exterior acoustics problems by the proposed technique. The contour plots of field solution for the real part of the potential for $ka=4\pi$ by adopting the proposed SMM, the FEM with DtN method,[29] and the BEM are shown in Figs. 15(a), 15(b), and 15(c),

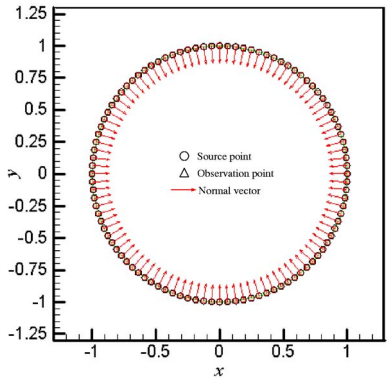

FIG. 8. (Color online) Nodes distribution (100 nodes) in Case 2.

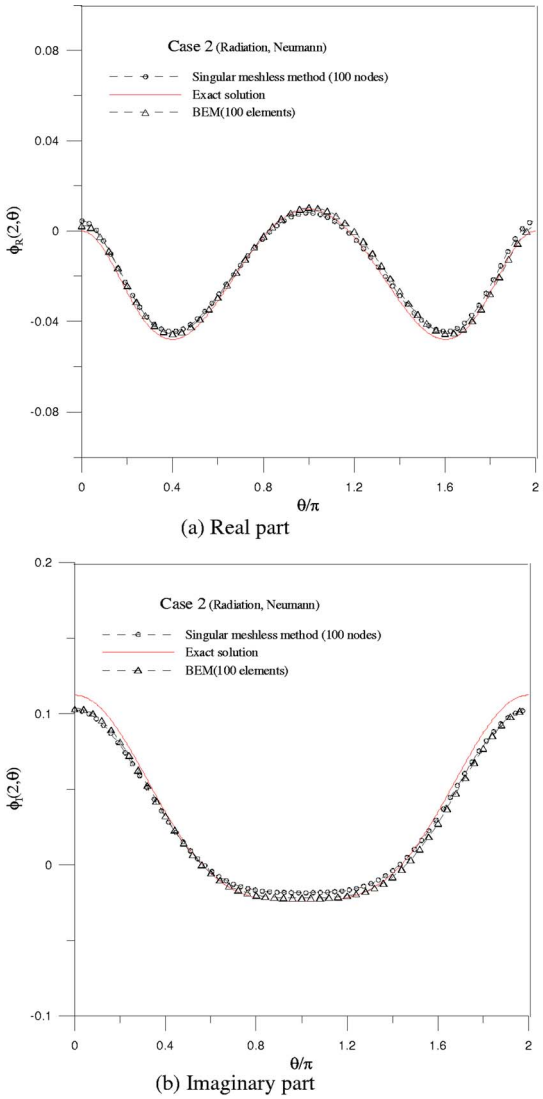

FIG. 9. Nonuniform radiation for a circular cylinder subject to Neumann BC in Case 2 for $ka=1$, $r=2a$: (a) real part, (b) imaginary part.

respectively. Figure 15 shows the better convergence of the present solution in comparison with the other two numerical solutions, BEM and DtN FEM.

V. CONCLUSIONS

In this study, we implement a singular meshless method using double layer potentials to solve radiation and scattering problems in two dimensions. Only the boundary nodes on the real boundary are required. The major difficulty of the coincidence of the source and collocation points that causes singularity in the conventional MFS is circumvented. The finite values of the diagonal terms for the influence matrices have been subtracted off by the proposed regularization technique to regularize the singularity and hypersingularity of the kernel functions, when the source and boundary points are coincident. The numerical results obtained by using the presented SMM for the three examples match very well with the analytical solutions and other numerical solutions using con-

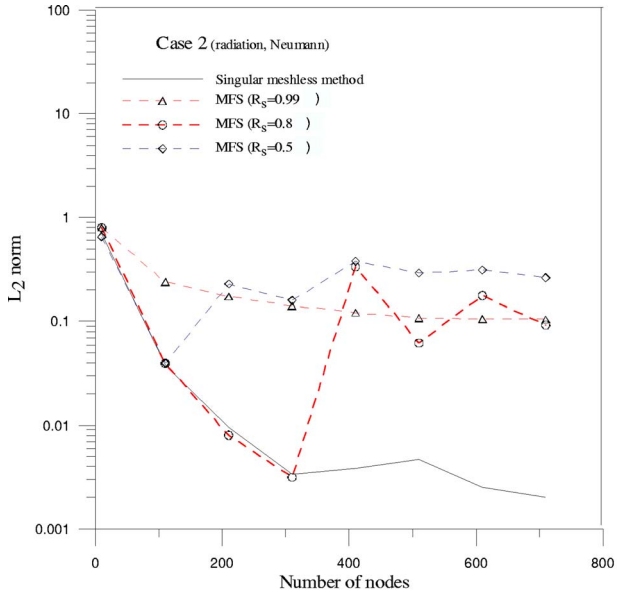

FIG. 10. (Color online) Comparison of error norms using the conventional MFS and proposed SMM for Case 2.

ventional MFS, BEM, or DtN FEM. A much simpler meshless numerical method is claimed as far as modeling of 2D exterior acoustics is concerned.

ACKNOWLEDGMENTS

Financial support from the National Taiwan University, and from the National Science Council of Taiwan under Grant No. NSC-92-2281-E-002-020, are gratefully appreciated. We would like to thank Professor A. S. Muleshkov of the University of Nevada at Las Vegas for discussing and editing the manuscript when D.L.Y. visited the Department of Mathematical Sciences at UNLV. We are also very grateful for constructive comments by the referees to improve our paper.

APPENDIX A: THE DETAILED DERIVATIONS OF EQS. (20) and (21)

The null-fields of the boundary integral equations (BIEs) based on the direct method are

$$0 = \int_B \frac{\partial \Phi^{(e)}(s,x^i)}{\partial n_s} \phi(s) dB(s) - \int_B \Phi^{(e)}(s,x^i) \frac{\partial \phi(s)}{\partial n_s} dB(s), \quad x^i \in D^e, \tag{A1}$$

$$0 = \int_B \frac{\partial^2 \Phi^{(e)}(s,x^i)}{\partial n_s \partial_{x^i}} \phi(s) dB(s) - \int_B \frac{\partial \Phi^{(e)}(s,x^i)}{\partial n_{x^i}} \frac{\partial \phi(s)}{\partial n_s} dB(s), \quad x^i \in D^e, \tag{A2}$$

where the superscript e denotes the exterior domain, Φ is the single layer potential, and is equal to $\ln(r_{ij})$ for the 2D Laplace problem. Let $[\partial \Phi^{(e)}(s,x^i)]/\partial n_s = \bar{A}^{(e)}(s,x^i)$, and $[\partial^2 \Phi^{(e)}(s,x^i)]/\partial n_s \partial n_{x^i} = \bar{B}^{(e)}(s,x^i)$. By employing the simple test method ($\partial \phi(s)/\partial n_s = 0$ when $\phi(s) = 1$), we can write Eqs. (A1) and (A2) as follows:

$$\int_B \bar{A}^e(s,x^i) dB(s) = 0 \quad x^i \in D^e, \tag{A3}$$

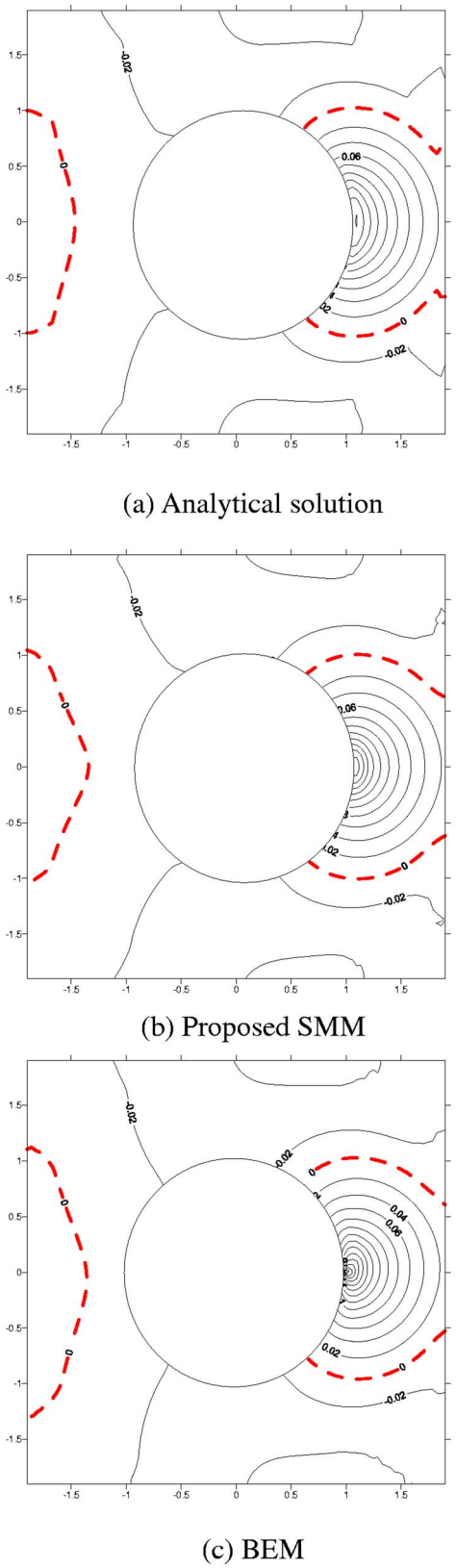

FIG. 11. (Color online) The contour plots for the real-part solutions in Case 2: (a) analytical solution, (b) proposed SMM (100 nodes), (c) BEM (100 elements).

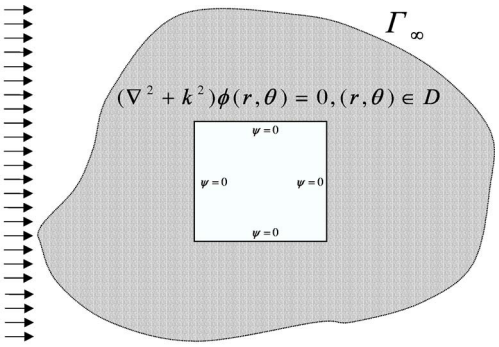

FIG. 12. The scattering problem for a square rod subject to Neumann BC in Case 3.

$$\int_B \bar{B}^e(s,x^i)dB(s) = 0, \quad x^i \in D^e. \tag{A4}$$

When the field point x^i approaches the boundary, we can discretize Eqs. (A3) and (A4) as follows:

$$\sum_{j=1}^{N} \bar{A}^{(e)}(s^j,x^i)\ell^j = 0, \quad x^i \in B, \tag{A5}$$

$$\sum_{j=1}^{N} \bar{B}^{(e)}(s^j,x^i)\ell^j = 0, \quad x^i \in B, \tag{A6}$$

where ℓ^j is the half distance of the $(j-1)$th source point and the $(j+1)$th source point. When the distribution of nodes is uniform, we are able to reduce Eqs. (A5) and (A6) to the following:

$$\sum_{j=1}^{N} \bar{A}^{(e)}(s^j,x^i) = 0, \quad x^i \in B, \tag{A7}$$

$$\sum_{j=1}^{N} \bar{B}^{(e)}(s^j,x^i) = 0, \quad x^i \in B, \tag{A8}$$

where

$$\bar{A}^{(e)}(s^j,x^i) = \frac{\partial \Phi^{(e)}(s^j,x^i)}{\partial n_s} = \frac{n_k y_k}{r_{ij}^2}, \tag{A9}$$

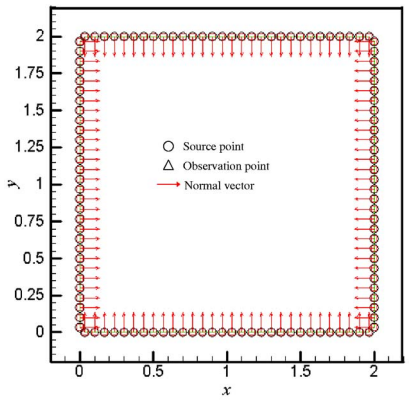

FIG. 13. (Color online) Nodes distribution (120 nodes) in Case 3.

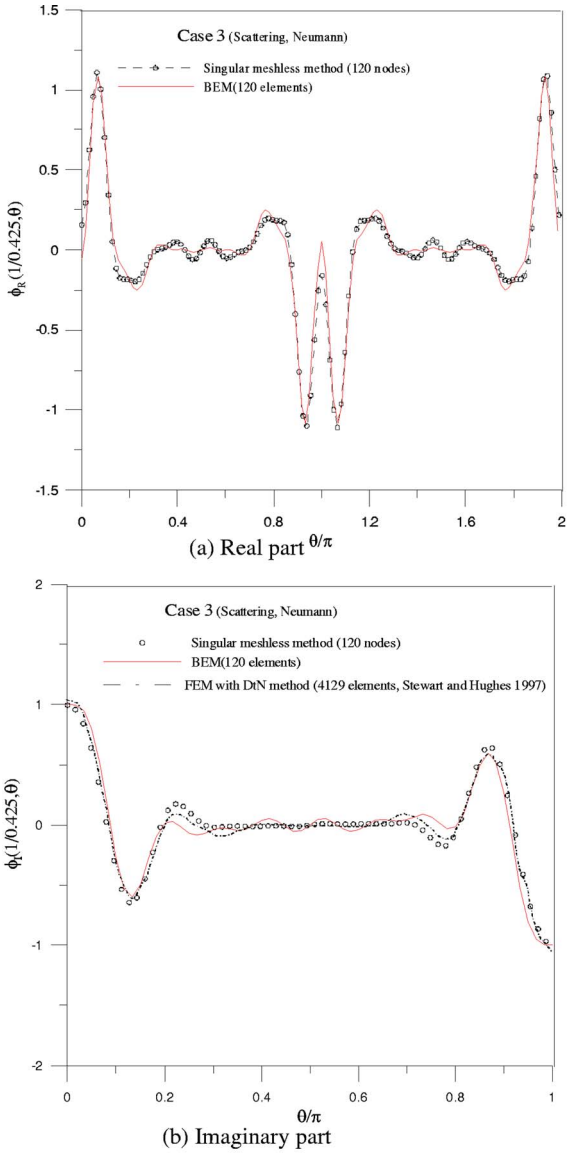

FIG. 14. (Color online) Plane wave scattering for a square rod subject to Neumann BC in Case 3 for $ka=4\pi$, $r=0.425$: (a) real part, (b) imaginary part (only the top half of the boundary is plotted).

$$\bar{B}^{(e)}(s^j,x^i) = \frac{\partial^2 \Phi^{(e)}(s^j,x^i)}{\partial n_{sj} \partial n_{x^i}} = 2\frac{y_k y_l n_k \bar{n}_l}{r_{ij}^4} - \frac{n_k \bar{n}_k}{r_{ij}^2}, \tag{A10}$$

which are Eqs. (20) and (21) in the text of Sec. III.

APPENDIX B: ANALYTICAL DERIVATION OF DIAGONAL COEFFICIENTS OF INFLUENCE MATRICES FOR CIRCULAR DOMAIN USING SEPARABLE KERNELS AND CIRCULANTS

By adopting the addition theorem, in a special case of the circular domain the two kernels in Eqs. (12) and (13) are expanded into separable kernels which segregate the field point, x, and source point, s, as follows:[2]

$$A^e(s,x) = \sum_{m=-\infty}^{\infty} \frac{\pi k}{2}[-iJ_m(k\rho) + Y_m(k\rho)] \times J'_m(kR)\cos(m(\theta-\varphi)), \quad \rho > R, \tag{B1}$$

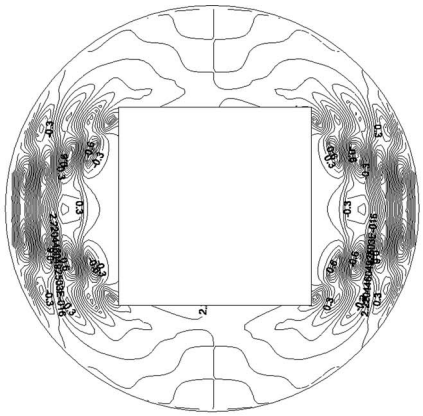

(a) Proposed SMM

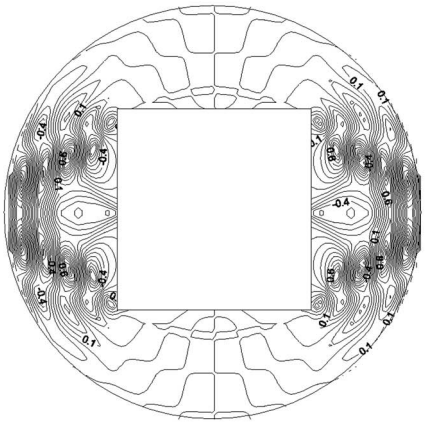

(b) BEM

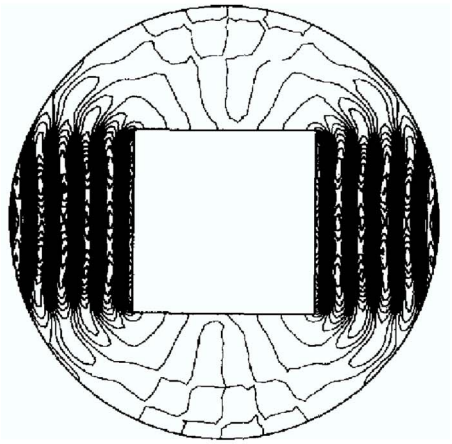

(c) FEM

FIG. 15. The contour plots for the real-part solutions in Case 3: (a) proposed SMM (120 nodes), (b) BEM (120 elements), (c) FEM with DtN method [4129 elements, Stewart and Hughes (1997)].

$$B^e(s,x) = \sum_{m=-\infty}^{\infty} \frac{\pi k}{2}[-i \times J'_m(k\rho) + Y'_m(k\rho)]J'_m(kR)\cos(m(\theta-\varphi)), \quad \rho > R, \tag{B2}$$

where $s=(R,\theta)$ and $x=(\rho,\varphi)$ in polar coordinates and the superscript denotes the derivative operator. Since the rotation symmetry is preserved for a circular boundary, the two influence matrices in Eqs. (8) and (9) are circulants with the elements

$$K_{ij} = K(R,\theta_j;\rho,\varphi_i), \tag{B3}$$

where the kernel K can be A^e or B^e in Eqs. (8) and (9) for the exterior problem, θ_j, φ_i are the angles of collocation and source points, respectively. By superimposing N lumped strength along the boundary, we have the influence matrices,

$$[K] = \begin{bmatrix} k_0 & k_1 & \cdots & k_{N-1} \\ k_{N-1} & k_0 & \cdots & k_{N-2} \\ \vdots & \vdots & \ddots & \vdots \\ k_1 & k_2 & \cdots & k_0 \end{bmatrix}, \tag{B4}$$

where the elements of the first row can be obtained from

$$k_j = K(R,\theta_j;\rho,0), \tag{B5}$$

in which $\varphi=0$ is set without loss of generality. The matrix $[K]$ in Eq. (A4) is found to be a circulant, since the rotational symmetry for the influence coefficients is observed. By introducing the following bases for the circulants, I, $(C_N)^1$, $(C_N)^2,\ldots$, and $(C_N)^{N-1}$, we can expand $[K]$ into

$$[K] = k_0 I + k_1 (C_N)^1 + k_2 (C_N)^2 + \cdots + k_{N-1}(C_N)^{N-1}, \tag{B6}$$

where I is the unit matrix and

$$C_N = \begin{bmatrix} 0 & 1 & 0 & \cdots & 0 & 0 \\ 0 & 0 & 1 & \cdots & 0 & 0 \\ \vdots & \vdots & \vdots & \ddots & \vdots & \vdots \\ 1 & 0 & 0 & \cdots & 0 & 0 \end{bmatrix}_{N\times N}. \tag{B7}$$

Based on the circulant theory, the eigenvalues for the influence matrix, $[K]$, are found as follows:

$$\lambda_l = k_0 + k_1\alpha_l + k_2(\alpha_l)^2 + \cdots + k_{2N-1}(\alpha_l)^{N-1}, \quad l = 0,1,2,\ldots,(N-1), \tag{B8}$$

where λ_l and α_l are the eigenvalues of $[K]$ and $[C_N]$, respectively. It is found that the eigenvalues of the circulants $[C_N]$ are the roots of $\alpha^N=1$, as shown in the following:

$$\alpha_l = e^{i(2\pi l/N)} \quad l = 0,1,2,\ldots,N-1. \tag{B9}$$

Substituting Eq. (B9) into Eq. (B8), we obtain

$$\lambda_l = \sum_{m=0}^{N-1} k_m \alpha_l^m = \sum_{m=0}^{N-1} k_m e^{i(2\pi ml/N)}, \quad l = 0,1,2,\ldots,(N-1). \tag{B10}$$

According to the definition of k_m in Eq. (B5), we have

$$k_m = k_{N-m}, \quad m = 0,1,2,\ldots,N-1. \tag{B11}$$

Substitution of Eq. (B11) into Eq. (B10) yields

$$\lambda_l = k_0 + \sum_{m=1}^{N-1} k_m(\alpha_l^m + \alpha_l^{N-m})$$

$$= \sum_{m=0}^{N-1} k_m \cos\left(\frac{2\pi ml}{N}\right), \quad l = 0,1,2,\ldots,N-1. \tag{B12}$$

By setting $\varphi=0$, without loss of generality, the Riemann sum reduces to the following integral:

$$\lambda_l = \frac{1}{\Delta\theta} \lim_{N\to\infty} \sum_{m=0}^{N-1} K(m\Delta\theta,0)\cos(ml\Delta\theta)\Delta\theta$$

$$= \frac{N}{2\pi}\int_0^{2\pi} \cos(l\theta)K(\theta,0)d\theta, \tag{B13}$$

where $\Delta\theta=2\pi/N$.

By employing the separable kernel $A^e(s,x)$ for exterior problem ($R<\rho$) in Eq. (B1) and the orthogonal conditions, Eq. (B13) then reduces to

$$\lambda_l = \pi k\frac{N}{2}[-iJ_l(k\rho) + Y_l(k\rho)]$$

$$\times J_l'(kR), \quad l = 0,1,2,3,\ldots,N-1. \tag{B14}$$

Similarly, we have

$$\upsilon_l = \pi k^2\frac{N}{2}[-iJ_l'(k\rho) + Y_l'(k\rho)]$$

$$\times J_l'(kR), \quad l = 0,1,2,3,\ldots,N-1 \tag{B15}$$

where λ_l and υ_l are the eigenvalues of $[A^e]$ and $[B^e]$, respectively.

Employing the invariant property of the influence matrices, the first invariant is the sum of all the eigenvalues. The diagonal coefficients of the two matrices for the exterior problem are obtained by the addition of all eigenvalues and are shown as

$$Na_{jj} = \sum_{l=0}^{N-1} \lambda_l, \tag{B16}$$

$$Nb_{jj} = \sum_{l=0}^{N-1} \upsilon_l. \tag{B17}$$

Substituting Eqs. (B14) and (B15) into Eqs. (B16) and (B17), we obtain

$$a_{jj} = -\frac{ik\pi}{4}\sum_{l=0}^{N-1} H_l^{(1)}(kR)[J_{l-1}(kR) - J_{l+1}(kR)], \tag{B18}$$

$$b_{jj} = -\frac{ik^2\pi}{4}\sum_{l=0}^{N-1} [H_{l-1}^{(1)}(kR) - H_{l+1}^{(1)}(kR)][J_{l-1}(kR)$$

$$- J_{l+1}(kR)]. \tag{B19}$$

Applying the addition theorem for the Bessel function, the limiting forms for small argument and approaching the collocation point to the source point, we obtain

$$\lim_{N\to\infty}\left(-\frac{4kR\pi}{N} + \frac{2Ni}{kR\pi}\right) = \lim_{N\to\infty}\sum_{l=0}^{N-1} H_l^{(1)}(kR)[J_{l-1}(kR)$$

$$- J_{l+1}(kR)]. \tag{B20}$$

Hence, the diagonal elements are easily determined from Eqs. (B18) and (B19) as follows:

$$a_{jj} = \frac{\pi}{\frac{2\pi R}{N}}, \quad N \gg 1. \tag{B21}$$

Similarly, we have

$$b_{jj} = \frac{(1+N)N}{8R^2} + \frac{\pi k^2}{4}i, \quad N \gg 1. \tag{B22}$$

It is worth noticing that diagonal terms for general domains of Eqs. (22) and (23) are analogous to Eqs. (B21) and (B22) for the special circular domain.

[1] S. Li and W. K. Liu, "Meshfree and particle methods and their application," Appl. Mech. Rev. **55**(1), (2002).

[2] T. Belytschko, L. Gu, and Y. Lu, "Fracture and crack growth by element-free Galerkin methods," Modell. Simul. Mater. Sci. Eng. **2**, 519–534 (1994).

[3] J. T. Chen, S. R. Kuo, K. H. Chen, and Y. C. Cheng, "Comments on vibration analysis of arbitrary shaped membranes using non-dimensional dynamic influence function," J. Sound Vib. **235**, 156–171 (2000).

[4] J. T. Chen, M. H. Chang, K. H. Chen, and S. R. Lin, "The boundary collocation method with meshless concept for acoustic eigenanalysis of two-dimensional cavities using radial basis function," J. Sound Vib. **257**, 667–711 (2002).

[5] J. T. Chen, M. H. Chang, and K. H. Chen, "Boundary collocation method for acoustic eigenanalysis of three-dimensional cavities using radial basis function," Comput. Mech. **29**, 392–408 (2002).

[6] J. T. Chen, I. L. Chen, and C. S. Wu, "On the equivalence of MFS and Trefftz method for Laplace problems," Proceedings of the Global Chinese Workshop on Boundary Element and Meshless Method, Hebei, China, 2003.

[7] J. T. Chen, C. S. Wu, Y. T. Lee, and K. H. Chen, "On the equivalence of the Trefftz method and method of fundamental solutions for Laplace and biharmonic equations," Comput. Math. Appl. (to be published).

[8] J. T. Chen, I. L. Chen, K. H. Chen, Y. T. Yeh, and Y. T. Lee, "A meshless method for free vibration of arbitrarily shaped plates with clamped boundaries using radial basis function," Eng. Anal. Boundary Elem. **28**, 535–545 (2005).

[9] W. Chen and M. Tanaka, "A meshfree, integration-free and boundary-only RBF technique," Comput. Math. Appl. **43**, 379–391 (2002).

[10] W. Chen and Y. C. Hon, "Numerical investigation on convergence of boundary knot method in the analysis of homogeneous Helmholtz, modified Helmholtz and convection-diffusion problems," Comput. Methods Appl. Mech. Eng. **192**, 1859–1875 (2003).

[11] G. Fairweather and A. Karageorghis, "The method of fundamental solutions for elliptic boundary value problems," Adv. Comput. Math. **9**, 69–95 (1998).

[12] R. A. Gingold and J. J. Maraghan, "Smoothed particle hydrodynamics: Theory and applications to non-spherical stars," Man. Not. Astro. Soc. **181**, 375–389 (1977).

[13] M. A. Golberg and C. S. Chen, "The method of fundamental solution for potential, Helmholtz and diffusion problems," in *Boundary Integral Methods-Numerical and Mathematical Aspects*, edited by M. A. Golberg (Computational Mechanics, 1998) pp. 103–176.

[14] S. W. Kang, J. M. Lee, and Y. J. Kang, "Vibration analysis of arbitrary shaped membranes using non-dimensional dynamic influence function," J. Sound Vib. **221**, 117–132 (1999).

[15] S. W. Kang and J. M. Lee, "Application of free vibration analysis of membranes using the non-dimensional dynamic influence function," J. Sound Vib. **234**, 455–470 (2000).

[16] W. K. Liu, S. Jun, S. Li, J. T. Adee, and T. Belyschko, "Reproducing kernel particle methods for structural dynamics," Int. J. Numer. Methods

Eng. **38**, 1655–1679 (1995).
[17]C. C. Tsai, D. L. Young, and A. H. D. Cheng, "Meshless BEM for three-dimensional Stokes flows," Comput. Model. Eng. Sci. **3**, 117–128 (2002).
[18]Y. S. Smyrlis and A. Karageorghis, "Some aspects of the method of fundamental solutions for certain harmonic problems," J. Sci. Comput. **16**, 341–371 (2001).
[19]D. L. Young, C. C. Tsai, T. I. Eldho, and A. H. D. Cheng, "Solution of Stokes flow using an iterative DRBEM based on compactly-supported, positive definite radial basis function," Comput. Math. Appl. **43**, 607–619 (2002).
[20]D. L. Young, K. H. Chen, and C. W. Lee, "Novel meshless method for solving the potential problems with arbitrary domains," J. Comput. Phys. **209**, 290–321 (2005).
[21]K. E. Atkinson, *The Numerical Solution of Integral Equations of the Second Kind*, 1st ed. (Cambridge University Press, Cambridge, 1997).
[22]M. Guiggiani, "Formulation and numerical treatment of boundary integral equations with hypersingular kernels," in V. Sladek and J. Sladek, editors, *Singular Integrals in Boundary Element Methods* (Computational Mechanics, 1998), Chap. 3, pp. 85–124.
[23]M. Guiggiani, G. Krishnasamy, T. J. Rudolphi, and F. J. Rizzo, "A general algorithm for the numerical solution of hypersingular boundary integral equations," ASME J. Appl. Mech. **59**, 604–614 (1992).
[24]*Singular Integrals in Boundary Element Methods*, edited by V. Sladek and J. Sladek (Computational Mechanics, Southampton, 1998).
[25]M. Tanaka, V. Sladek, and J. Sladek, "Regularization techniques applied to boundary element methods," Appl. Mech. Rev. **47**, 457–499 (1994).
[26]I. Harari, P. E. Barbone, M. Slavutin, and R. Shalom, "Boundary infinite elements for the Helmholtz equation in exterior domains," Int. J. Numer. Methods Eng. **41**, 1105–1131 (1998).
[27]F. Ihlenburg, *Finite Element Analysis of Acoustic Scattering*, Applied Mathematical Sciences (Springer, Berlin, 1998), p. 132.
[28]M. Abramowitz and I. A. Stegun, *Handbook of Mathematical Functions with Formulation Graphs and Mathematical Tables* (Dover, New York, 1972).
[29]J. R. Stewart and T. J. R. Hughes, "*h*-adaptive finite element computation of time-harmonic exterior acoustics problems in two dimensions," Comput. Methods Appl. Mech. Eng. **146**, 65–89 (1997).